OPTIMAL DESIGN AND ASSESSMENT OF HIGH PERFORMANCE MICRO BARE-TUBE HEAT EXCHANGERS

Nobuhide Kasagi[1]**, Yuji Suzuki**[1]**, Naoki Shikazono**[1] **and Tomohisa Oku**[2]

[1] The University of Tokyo, Hongo 7-3-1, Bunkyo-ku, Tokyo, 113-8656, Japan; E-mail: shika@thtlab.t.u-tokyo.ac.jp
[2] Nissan Motor Co., Ltd., Okatsukoku 560-2, Atsugi-shi, Kanagawa 243-0126, Japan; E-mail: oku09@pop02.odn.ne.jp

ABSTRACT

An optimal design methodology is proposed for micro bare-tube heat exchangers. A simulated annealing method is employed with a trained neural network representing the heat transfer and pressure drop characteristics of a specified tube bank. A commercial CFD code, FLUENT5, is used to obtain the heat transfer and pressure drop data sets for in-line tube bundles, which are then used to train the neural network. Three types of micro bare-tube heat exchangers are designed and compared to conventional commercial heat exchangers. The optimized micro bare-tube heat exchangers show better performance than conventional gas-liquid heat exchangers.

INTRODUCTION

Great efforts have been made for heat transfer augmentation, and a number of compact heat exchanger designs have been proposed to date (e.g., Kays and London, 1984). Most of the compact gas-liquid heat exchangers utilize fins in order to compensate a lower heat transfer rate on the gas side. Paitoonsurikarn et al. (2000) proposed a micro bare-tube heat exchanger, which was composed of a bundle of small diameter tubes without conventional fins. It was shown that the micro bare-tube heat exchanger had a possibility of improving heat transfer performance and compactness with its high over-all heat transfer rate and large heat transfer area density.

One of the major reasons for achieving such high heat transfer performance is that the heat resistance of the fin and that of the inner-tube can be ignored. In general, however, these good features result in a large pressure drop, which causes large pumping power and also fan noise. Since the density and thermal conductivity of air are generally smaller than those of the liquid inside the tube, the air-side design becomes the major concern. The trade-off mentioned above requires large efforts when designing compact heat exchangers. Thus, it is important to estimate accurately both heat transfer rate and pressure drop of the air-side flow.

Paitoonsurikarn et al. (2000) utilized the heat transfer and pressure drop correlations proposed by Zukauskas (1972). However, those correlations are not verified for predicting a wide range of tube arrangements and also at low Reynolds numbers, e.g., Re < 500, which is a characteristic Re range for compact heat exchangers. The main objective of this study is to propose a reliable optimization method for designing micro bare-tube heat exchangers. Then, the proposed method is applied to three types of heat exchangers, and the optimized designs are assessed in comparison with conventional commercial heat exchangers.

In the present paper, numerical simulation of the flow through in-line tube bundles was first carried out in order to accumulate heat transfer and pressure drop data. A commercial CFD code, FLUENT5, was employed to calculate the flow and thermal field around in-line tube bundles. Since it is not easy to correlate well the effects of important parameters such as transverse and longitudinal tube pitches and Reynolds number in a simple algebraic expression, a neural network is introduced to interpolate the obtained Nusselt numbers and pressure loss coefficients. Then, the micro bare tube heat exchanger is optimized with a simulated annealing (SA) method using the trained neural network representing the heat transfer and pressure drop characteristics of a specified tube bank. The SA method prevents the result from falling onto a local optimal point, and is preferable for designing heat exchangers of new configurations.

Three types of micro bare-tube heat exchangers are optimized and compared to conventional commercial heat exchangers. They are automobile heat exchangers, electronic equipment coolers, and gas turbine recuperators.

NUMERICAL SIMULATION OF FLOW AROUND IN-LINE TUBE BUNDLES

A commercial CFD code, FLUENT5, is employed to calculate the flow and thermal field around in-line tube bundles with three rows in the transverse direction and 10 columns in the longitudinal direction as shown in Fig. 1. The tube surface is assumed to be isothermal. Periodic boundary condition is employed in the transverse direction, and uniform velocity and free outflow conditions are given at inlet and outlet boundaries, respectively. The temperature dependence of the physical properties of working fluids is neglected.

The Reynolds number based on the tube diameter and the maximum velocity at the minimum cross section, Re_{max}, is varied in the range of Re_{max}=10 to 300. The dimensionless transverse and longitudinal tube pitches, P_T

Proc. 4th Int. Conf. on Compact Heat Exchangers and Enhancement Technologies for the Process Industries, Crete, Sep. 29-Oct 3, 2003, pp. 241-246.

and P_L, are varied from 1.25 to 1.4. In total, 46 cases are calculated. It is known that three dimensionality of the flow is observed in the case of a single cylinder around Re_{max} =100. In the present study, however, two-dimensional unsteady calculation is performed because it is considered that the effect of three dimensionality of the flow on the mean heat transfer and pressure drop is negligibly small.

Finally, the Nusselt number Nu_i and the pressure coefficient C_p at i-th column are obtained by time averaging over several vortex shedding periods of a single cylinder at the same condition.

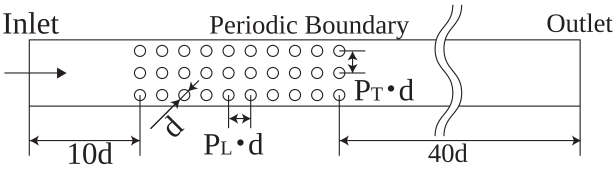

Fig. 1 Computational Domain.

NEURAL NETWORK DATABASE

In order to obtain the optimal design of micro bare-tube heat exchangers, it is needed to interpolate accurately both heat transfer rate and pressure drop for wide ranges of tube pitches P_T, P_L and also of Re_{max}. It is not easy to correlate the CFD results with a simple algebraic expression. Thus, a neural network is employed to construct the heat transfer and pressure drop database from the CFD results.

Figure 2 shows the neural network structure proposed in this study. It is composed of three sub networks, NN1, NN2 and NN3. Input data are the tube pitches P_T, P_L and the Reynolds number Re_{max}, which is based on the tube diameter and the maximum bulk mean velocity at the narrowest cross section in between two tubes. The final output data are the Nusselt number and the pressure coefficient C_p. Sub neural network NN1 first outputs the Nusselt number and the drag coefficient of the first column, Nu_1 and C_{D1}, and then these values are used as the input data for the second sub neural network of NN2. Sub neural network NN2 outputs Nu and C_D of the second column, and again those data are utilized as the input data for calculating the next downstream column. This iteration is repeated

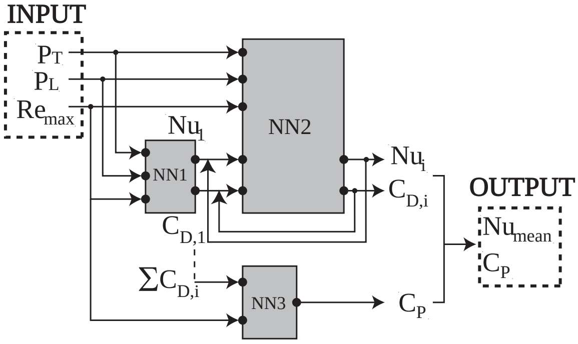

Fig. 2 Diagram of the Neural Network.

until NN2 reaches the final column, and finally sub network NN3 calculates the averaged Nusselt number Nu_{mean} and the sum of drag coefficients C_p=ΣC_{Di}.

In the present study, a three layer neural network with the sigmoid activation function is employed. The number of neurons in the hidden layer is 3, 4 and 2 for NN1, NN2, and NN3, respectively. Synaptic weights are optimized using the backward propagation algorithm with a steepest gradient method. All 46 data points for various pitches and Reynolds numbers are used as a training data set.

Figures 3 and 4 show Nu_{mean} and C_p at Re_{max} =300 predicted by the neural network. The black dots denote the data points obtained by CFD. Both Nu_{mean} and C_p show an abrupt increase around P_L=2.0. This is because the flow pattern changes from steady to oscillating unsteady states. This transition is found to occur at larger P_L as the Reynolds number decreases. As the transverse tube pitch of P_T becomes smaller, C_p increases drastically around P_T=1.5, while Nu shows only a moderate increase. The flow is greatly accelerated at the narrow cross section between the tubes, and thus the dynamic pressure loss becomes large.

The flow inside the tube is found to be in the laminar Re range for all the cases considered in this study. Thus, the heat transfer rate inside the tube is given by the analytical solution of Nusselt number under the isothermal condition:

$$Nu_{in} = \frac{h_{in} d_{in}}{k_{in}} = 3.66 \,. \qquad (1)$$

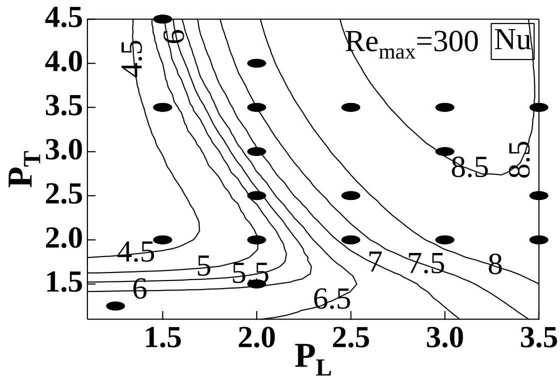

Fig. 3 Contour of Nu_{mean} at Re_{max} =300.

Re_{max}=300

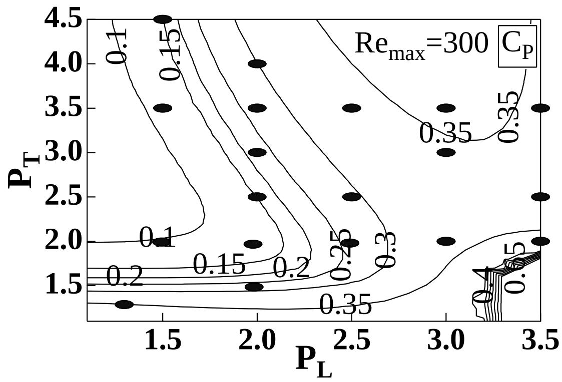

Fig. 4 Contour of C_p at Re_{max} =300.

The pressure drop of flow inside the tube is calculated by the following formula given by Kays and London (1984):

$$\Delta p_{core} = \frac{\rho u_m^2}{2}\left(K_c + K_e + f\,\frac{l}{d_{in}}\right), \qquad (2)$$

where f=64/Re_{in} is the friction factor, and K_c and K_e are the entrance and exit pressure loss coefficients, respectively. Those values for K_c and K_e are found in Kays and London (1984). The total pressure drop including the pressure drop at inlet and outlet manifolds is assumed to be three times the core pressure drop, i.e., $\Delta p_{in}=3\Delta p_{core}$.

OPTIMAL DESIGN BY SIMULATED ANNEALING

Twelve design parameters must be optimized for micro bare-tube heat exchangers, as shown in Fig. 5. Some of these parameters are prescribed as design conditions and the rest are optimized so as to maximize or minimize the cost function. The cost functions for tested heat exchangers are as follows.

Automobile Heat Exchangers

- Case 1: Minimization of pumping power. Heat exchange rate and volume are fixed.
- Case 2: Maximization of heat exchange rate. Pumping power and volume are fixed.
- Case 3: Minimization of core volume. Pumping power and heat exchange rate are fixed.

The specifications of tested heat exchangers are listed in Table 1. They are typical commercial automobile heat exchangers.

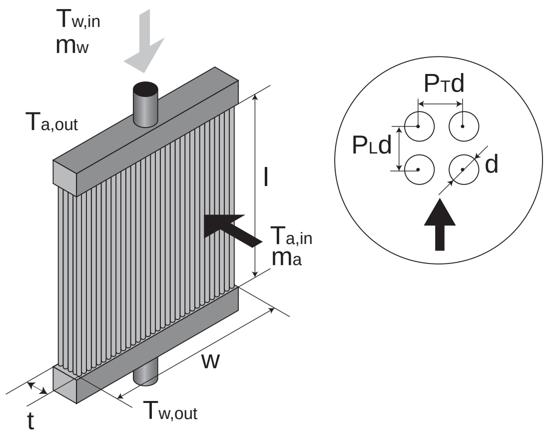

Fig. 5 Design Parameters of Micro Bare-Tube Heat Exchangers.

Electronic equipment cooling system

- Case 4: Minimization of pumping power. Heat exchange rate and volume are fixed

Micro gas turbine recuperator

- Case 5: Maximization of total system efficiency. Core volume is fixed

With a set of governing equations, design parameters are optimized by using the simulated annealing method in such a way that they should minimize the cost function described above. The number of temperature steps and the number of random steps per a temperature step are both chosen as 1000. The temperature of the system is decreased according to a logarithmic annealing schedule with an arbitrary high starting temperature.

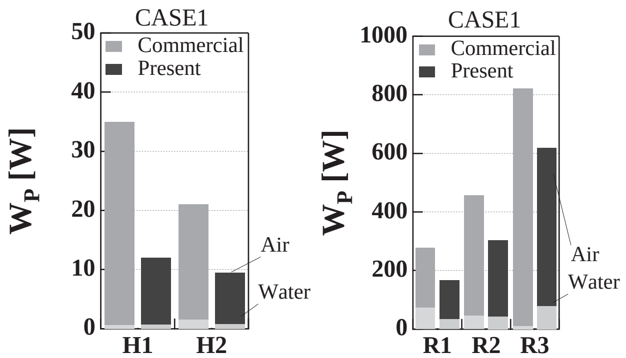

Fig. 6 Pumping Power for Optimized Design in Case 1.

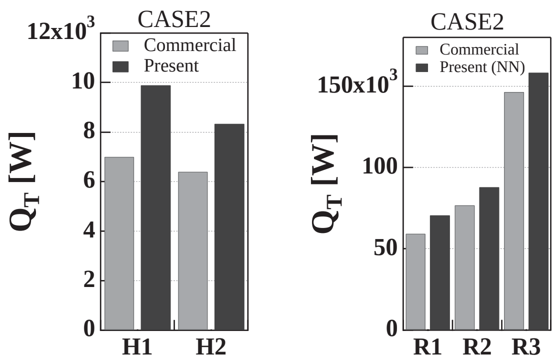

Fig. 7 Total Heat Exchange Rate for Optimized Design in Case 2.

Table 1. Specifications of commercial automobile heat exchangers.

	Definition	Q (kW)	W (W)	w (m)	l (m)	t (m)	Vol (m^3)	$T_{w,in}$ (°C)	$T_{a,in}$ (°C)	m_a (kg/s)	m_w (kg/s)	Δp_a (Pa)	Δp_w (kPa)	W_a (W)	W_w (W)
H1	Heater Core	7.0	35.0	0.20	0.15	0.035	0.001050	80.0	15.0	0.116	0.2	343	2.93	34.3	0.59
H2	Heater Core	6.4	21.0	0.20	0.15	0.025	0.000750	80.0	15.0	0.116	0.2	196	7.33	19.6	1.47
R1	Radiator	59.3	277.4	0.65	0.43	0.016	0.004472	80.0	20.0	1.624	2.0	147	36.0	206	72.0
R2	Radiator	76.8	456.2	0.65	0.43	0.027	0.007547	80.0	20.0	1.624	2.0	294	22.7	412	45.3
R3	Radiator	146.5	782.4	0.70	0.75	0.050	0.026250	80.0	20.0	3.050	2.0	294	4.93	811	10.1

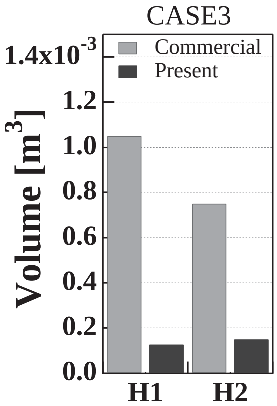

Fig. 8 Core Volume for Optimized Design in Case 3.

OPTIMAL DESIGNS OF MICRO BARE-TUBE HEAT EXCHANGERS

In this section, obtained optimal designs for heat exchangers will be shown. Figures 6, 7 and 8 show the comparison of optimal micro bare-tube heat exchangers and commercial ones for Cases 1, 2 and 3, respectively. It can be seen that the micro bare-tube heat exchanger shows large improvement over conventional heat exchangers especially for heater cores (H1 and H2). Heater cores H1 and H2 have relatively small frontal area ($w \times l$) and large thickness t compared to the radiators (R1, R2 and R3). The good feature of micro bare-tube heat exchanger, i.e., high heat transfer rate with low pressure drop, is very effective for such heat exchangers with small frontal areas.

One of the promising applications of micro bare-tube heat exchangers is the cooling system for electronic equipment. Semiconductor technologies have shown remarkable improvements over the decades, and the outlook of CPU power trend shows further increase. As a result, the cooling of those electronic devices is becoming crucial even for open server client systems. Figure 9 shows the schematic view of such cooling system. Heat is removed from the CPU by the cooling plate and transferred to the micro bare-tube heat exchanger by a single phase liquid. An aluminum block with a number of rectangular ducts is employed as a cooling plate in this study. The cost function is the sum of the pumping power of coolant and the fan input for the micro bare-tube heat exchanger in this case.

Figure 10 shows the total pumping power plotted against the heat exchange rate. The ratio of the heat exchanger core width, length and thickness are fixed as w:l:t=5:5:1. The value of a commercially available heat exchanger for a liquid cooling server is also plotted in the figure. It is shown that the micro bare-tube heat exchanger can drastically reduce the core volume for the same pumping power and heat exchange rate.

Another example is a recuperator for micro gas turbine. Figure 11 shows the schematic diagram of a recuperated gas turbine cycle. It is important to improve the recuperator temperature effectiveness ε_R, because it not only leads to a high system efficiency, but also can reduce the inlet temperatures of turbine and recuperator. Thus, the possibility of introducing a micro bare-tube heat exchanger as a micro turbine recuperator is examined here. In the preliminary study, it was found that the inner tube pressure drop was crucial for gas-gas micro bare-tube heat exchangers. Thus, the ratio of the heat exchanger core width, length and thickness are fixed as w:l:t=15:1:10 for this case. The turbine power output, the pressure ratio and the turbine inlet temperature are set as 5kW, π=3 and TIT=1000 $^{\mathrm{o}}$C , respectively.

Figures 12 and 13 show the recuperator temperature effectiveness, pressure drop and efficiency of the optimized system. The temperature effectiveness ε_R and the dimensionless total pressure drop $\Delta p/p$ are defined as follows,

$$\varepsilon_R = \frac{T_5 - T_2}{T_4 - T_2}, \tag{3}$$

$$\frac{\Delta p}{p} = \frac{p_2 - p_5}{p_2} + \frac{p_4 - p_6}{p_4}, \tag{4}$$

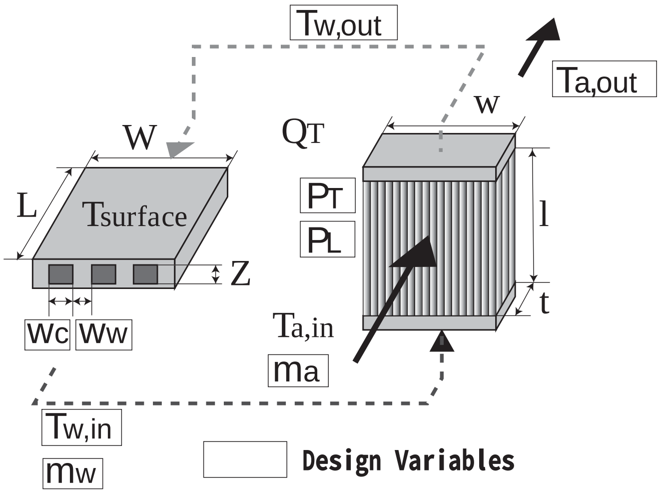

Fig. 9 Schematic View of Cooling System for Electronic Equipment (Case 4).

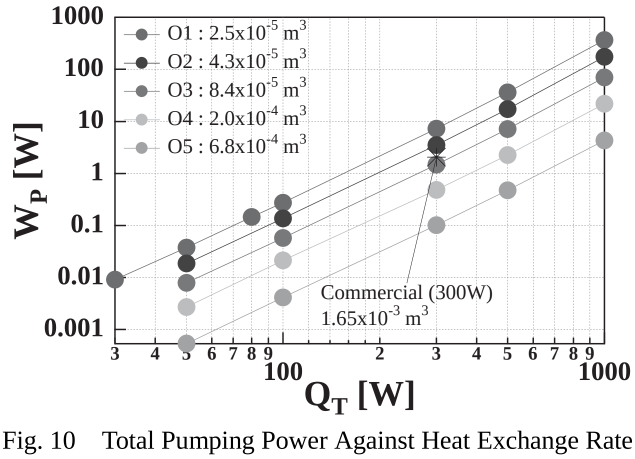

Fig. 10 Total Pumping Power Against Heat Exchange Rate at Various Core Volumes for Optimization Case 4.

Proc. 4th Int. Conf. on Compact Heat Exchangers and Enhancement Technologies for the Process Industries, Crete, Sep. 29-Oct 3, 2003, pp. 241-246.

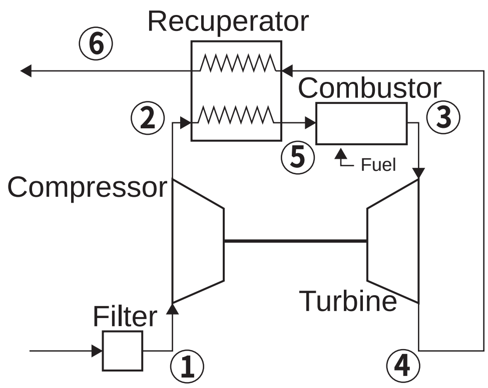

Fig. 11 Recuperated Gas Turbine Cycle (Case 5).

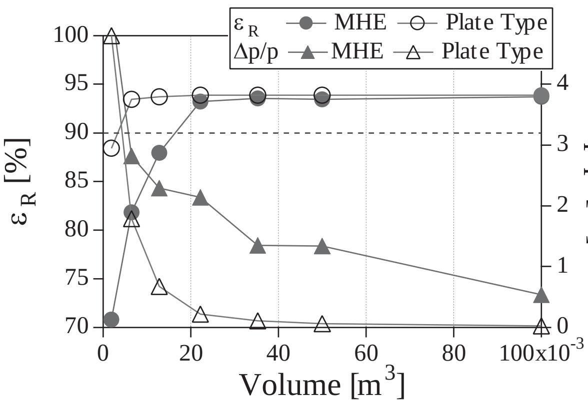

Fig. 12 Recuperator Temperature Effectiveness and Pressure Drop for Optimization Case 5.

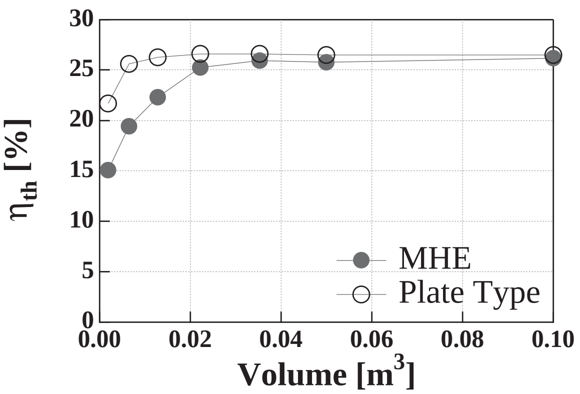

Fig. 13 System Efficiency for Optimization Case 5.

where the subscripts correspond to the locations in the gas turbine cycle described in Fig. 11. The system efficiency was calculated by the simulation code developed by Fukunaga (2000) and Uechi et al. (2001). Both compressor and turbine adiabatic efficiencies were set to be 80% in this case.

Comparison is made against a conventional counter flow plate heat exchanger with a cubic core. The micro bare-tube heat exchanger shows lower temperature effectiveness and larger pressure drop than the conventional plate heat exchanger, resulting in a lower system efficiency. This is attributed to the large pressure loss inside the tube. It is difficult to increase the in-tube cross section area with

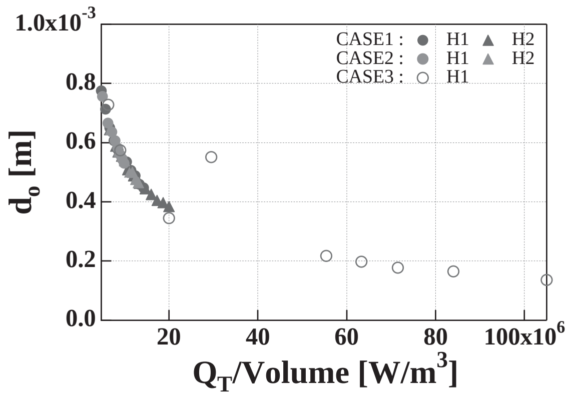

Fig. 14 Optimized Tube Diameter in Cases 1, 2, and 3.

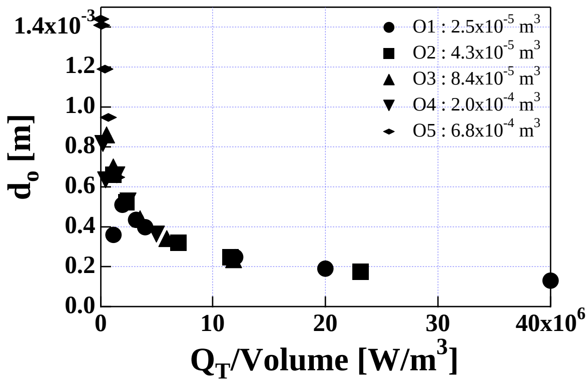

Fig. 15 Optimized Tube Diameter in Case 4.

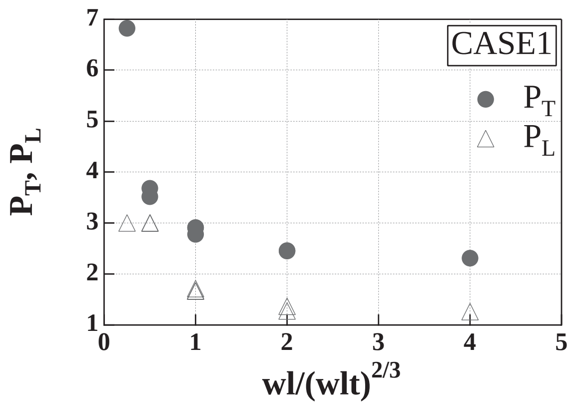

Fig. 16 Optimized Tube Pitch vs. Frontal Area in Case 1.

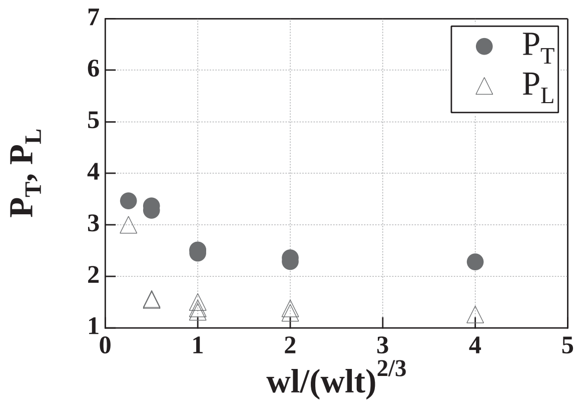

Fig. 17 Optimized Tube Pitch vs. Frontal Area in Case 4.

small diameter tubes.

DISCUSSION

For gas-liquid heat exchangers such as automobile heat exchangers and electronic equipment coolers, pumping power of the gas side generally dominates over that of the liquid side due to the density difference. Thus, the optimized specifications for the micro bare-tube heat exchangers are obtained so as to minimize the air side pressure drop, and the design parameters show systematical trend against design condition variations. The optimized tube diameter for Cases 1, 2, 3 and 4 are shown in Figs. 14 and 15. The optimized tube diameter data are well correlated on a single line. It asymptotes to a value around d_o=0.2mm as the heat load increases. This small tube diameter should be selected, because the pumping power inside the tube is negligibly small.

The optimized tube transverse and longitudinal pitches of P_T and P_L are plotted against the non-dimensionalized frontal area in Figs. 16 and 17. The optimized tube pitches asymptote to values around P_T=2.4 and P_L=1.3 as the frontal area increases. The flow pattern in this tube arrangement resembles to that inside parallel plates. As the optimized tube pitches are nearly constant, the heat exchanger area density is increased by introducing smaller diameter tubes when the heat load is increased.

For gas-gas heat exchangers such as gas turbine recuperators, the pumping power of both sides are nearly on the same order of magnitude. So, it is difficult to adopt small diameter tubes in this case, and this means that it is not feasible to construct compact gas-gas heat exchangers with micro bare tubes.

CONCLUSIONS

In the present study, the following conclusions are derived:

1. The Nusselt number and the pressure coefficient of micro bare-tube heat exchangers largely depend on the Reynolds number and the tube pitches, P_T and P_L. The data obtained by numerical simulation are correlated by a neural network composed of three sub-networks.
2. Three types of heat exchangers are optimized by the simulated annealing method. Since the tube diameter can be decreased for gas-liquid heat exchangers such as automobile heat exchangers and electronic equipment coolers, the micro bare-tube heat exchangers show large improvement over conventional heat exchangers. The optimized tube diameter decreases as the heat load increases. Also, the optimized transverse and longitudinal tube pitches are found to be around P_T=2.4 and P_L=1.3, respectively.
3. For gas-gas heat exchangers such as gas turbine recuperators, it is difficult to adopt small diameter tubes because the pumping power inside the tube cannot be ignored. Thus, it is not feasible to construct compact gas-gas heat exchangers with micro bare tubes.

ACKNOWLEDGEMENT

This work was supported through the Grant in Aid for Scientific Research (A) (No.13305015) by the Ministry of Education, Culture, Sports, Science and Technology (MEXT).

NOMENCLATURE

A Heat transfer area, m^2
C_D Drag coefficient, $\Delta p/\left(\rho u_{\max}^2/2\right)$
Cp Pressure coefficient, ΣC_D
d Tube diameter, m
f Friction factor, $64/\mathrm{Re}_{in}$
h Heat transfer rate, W/m^{2}K
k Thermal conductivity, W/mK
l Heat exchanger height, m
m Mass flow rate, kg/s
Nu Nusselt number, hd/k
p Pressure, Pa
P_T Transverse pitch
P_L Longitudinal pitch
Q Heat exchange rate, W
Re_{in} In-tube Reynolds number, $u_m d_{in}/\nu$
Re_{max} Reynolds number, $u_{max} d/\nu$
t Heat exchanger thickness, m
T Temperature, K
w Heat exchanger width, m
W Pumping power, W
π Pressure ratio, $P_{turbine,in}/P_{turbine,out}$
ε Recuperator temperature effectiveness
η System efficiency

Subscript

a air
i i-th column
in inner
m mean
out outer
R recuperator
w water

REFERENCES

Fukunaga, S. 2000, Study on Designing High Efficiency Micro Gas Turbines (in Japanese), BS Thesis, The University of Tokyo.

Kays, W. M. and London, A. L., 1984, *Compact Heat Exchangers 3rd edition*, John Wiley & Sons.

Paitoonsrikarn, S., Kasagi N. and Suzuki, Y., 2000, Optimal Design of Micro Bare-Tube Heat Exchanger, Proc. Symp. Energy Eng. in the 21st Century, Vol. 3, pp. 972-979.

Uechi, H., Kimijima, S. and Kasagi, N., 2001, Cycle Analysis of Gas Turbine-Fuel Cell Hybrid Micro Generation System, Proc. 2001 Int. Joint Power Generation Conference, New Orleans, Louisiana.

Zukauskas, A., 1972, Heat Transfer from Tubes in Cross Flow, Adv. in Heat Transfer, pp. 93-160.